

A Gravitational Mechanism for the Acceleration of Ultrarelativistic Particles

C. Chicone

*Department of Mathematics
University of Missouri-Columbia
Columbia, Missouri 65211, USA*

B. Mashhoon

*Department of Physics and Astronomy
University of Missouri-Columbia
Columbia, Missouri 65211, USA*

(Dated: November 5, 2018)

Abstract

Imagine a swarm of free particles near a point P outside a gravitating mass M and a free reference particle at P that is on a radial escape trajectory away from M . Relative to this reference particle and in a Fermi normal coordinate system constructed along its worldline, the particles in the swarm that move along the radial direction and are ultrarelativistic (that is, they have speeds above $c/\sqrt{2}$) decelerate toward this terminal speed. On the other hand, the swarm particles that are ultrarelativistic and move in directions normal to the radial (jet) directions accelerate to almost the speed of light by the gravitational tidal force of the mass M . The implications of these effects as well as the influence of the higher-order terms on the tidal acceleration mechanism are investigated. The observational evidence in support of these general relativistic effects is briefly discussed.

PACS numbers: 04.20.Cv, 97.60.Lf, 98.58.Fd, 98.70.Sa

I. INTRODUCTION

The geodesic deviation equation in general relativity is often compared with the Lorentz force law in electrodynamics. Both connect the corresponding fields to the mechanics of test particles and can thus be employed to provide operational definitions of the gravitational and electromagnetic fields, respectively. In terms of the dynamics of *ultrarelativistic* test particles, however, there is a fundamental difference between the two equations. To illustrate this difference, let us consider the motion of a test particle of mass m and charge q in an electromagnetic field (\mathbf{E}, \mathbf{B}) in Minkowski spacetime with inertial coordinates $x^\mu = (t, \mathbf{x})$,

$$\frac{d}{dt} \left(\frac{\mathbf{v}}{\sqrt{1-v^2}} \right) = \frac{q}{m} (\mathbf{E} + \mathbf{v} \times \mathbf{B}), \quad (1)$$

where $c = 1$ throughout this paper. This equation can be written as

$$\frac{d\mathbf{v}}{dt} = \frac{q}{m} \sqrt{1-v^2} [\mathbf{E} - (\mathbf{E} \cdot \mathbf{v})\mathbf{v} + \mathbf{v} \times \mathbf{B}]. \quad (2)$$

It is evident from this relation—as a result of the appearance of $\sqrt{1-v^2} = 1/\gamma$ as a factor on its right-hand side—that as $v \rightarrow 1$, it becomes very difficult to change the velocity of the test particle; that is, either the field should be maintained over a long integration time or the external electromagnetic field must become exceedingly strong. Otherwise, charged particles with v^2 extremely close to unity simply behave as essentially free particles and travel along a straight line. This may be interpreted in terms of the energy of the ultrarelativistic particle, i.e. $d(m\gamma)/dt = q\mathbf{E} \cdot \mathbf{v}$. For $v^2 \rightarrow 1$, the particle has enormous energy and any significant change in its velocity produces a significant change in the energy of the particle; therefore, unless an interaction with enormous energy is involved, the particle can be considered to be essentially free. Moreover, in the limit of a massless particle such that q/m remains finite as $m \rightarrow 0$, the particle simply follows a straight line at the speed of light, as expected. This situation should be contrasted with the well-known phenomenon of bending of a light ray in a gravitational field; therefore, the analogue of equation (2) must be fundamentally different for the gravitational interaction. In fact, we will demonstrate that the analogue of the $1/\gamma$ factor is absent in the gravitational case. For one-dimensional motion along a straight line, (2) reduces to

$$\frac{dv}{dt} = \frac{q}{m} (1-v^2)^{\frac{3}{2}} E_{\parallel}, \quad (3)$$

where E_{\parallel} is the component of the electric field along the direction of motion of the particle. The relevant factor in this case is $1/\gamma^3$; again, we will show that such a factor is remarkably

absent in the gravitational case.

Consider now the corresponding situation in a gravitational field. The analogue of equation (1) is the geodesic deviation equation. To express this equation in a form that can be compared with (1), we must establish a Fermi coordinate system about one of the geodesics [1]. In the curved spacetime of general relativity, such a coordinate patch is the closest analogue of the global inertial system employed in equation (1). Let $X^\mu = (T, \mathbf{X})$ be the Fermi coordinate system that is valid in a cylindrical spacetime region around the worldline of the reference geodesic observer \mathcal{O} . The motion of any other free test particle \mathcal{A} in this neighborhood is given by the geodesic equation in Fermi coordinates

$$\frac{d^2 X^\mu}{ds^2} + \Gamma_{\alpha\beta}^\mu \frac{dX^\alpha}{ds} \frac{dX^\beta}{ds} = 0, \quad (4)$$

where s is the proper time of \mathcal{A} and $\Gamma_{\alpha\beta}^\mu$ is the spacetime connection in Fermi coordinates. It is important to recognize that the reference geodesic remains fixed throughout our analysis. This approach to the deviation equation should be distinguished from the traditional one based on the Jacobi equation, which involves a certain linearization about the reference geodesic. Rather, we simply solve the geodesic equation in a Fermi normal coordinate system established along the reference geodesic.

Let us note that equations (1)–(3) are expressed with respect to the coordinate time t of the global inertial system; therefore, it is necessary, for the purposes of comparison, to write equation (4) in terms of the temporal Fermi coordinate T as follows:

$$\frac{d^2 T}{ds^2} + \Gamma_{\alpha\beta}^0 \frac{dX^\alpha}{ds} \frac{dX^\beta}{ds} = 0, \quad (5)$$

$$\frac{d^2 X^i}{ds^2} + \Gamma_{\alpha\beta}^i \frac{dX^\alpha}{ds} \frac{dX^\beta}{ds} = 0. \quad (6)$$

Using the identity

$$\frac{d^2 X^i}{ds^2} = \frac{d^2 T}{ds^2} \frac{dX^i}{dT} + \left(\frac{dT}{ds} \right)^2 \frac{d^2 X^i}{dT^2}, \quad (7)$$

equations (5)–(7) imply that

$$\frac{d^2 X^i}{dT^2} + \left(\Gamma_{\alpha\beta}^i - \Gamma_{\alpha\beta}^0 \frac{dX^i}{dT} \right) \frac{dX^\alpha}{dT} \frac{dX^\beta}{dT} = 0. \quad (8)$$

This is the analogue of equation (1) in the theory of gravitation, except that the geodesic worldline could in general be timelike, null or spacelike. To ensure that we are dealing with a *timelike* worldline, equation (4) must be supplemented with the requirement that

$$g_{\mu\nu} \frac{dX^\mu}{ds} \frac{dX^\nu}{ds} = -1, \quad (9)$$

which is preserved by (4) throughout the motion. Writing the four-velocity of \mathcal{A} in Fermi coordinates as

$$U^\mu = \Gamma(1, \mathbf{V}) \quad (10)$$

with $\mathbf{V} = d\mathbf{X}/dT$, equation (9) can be expressed as

$$\Gamma^{-2} = -g_{00} - 2g_{0i}V^i - g_{ij}V^iV^j. \quad (11)$$

Here $\Gamma = dT/ds$ is the modified Lorentz factor of particle \mathcal{A} , so that $\Gamma \rightarrow \infty$ indicates that $ds \rightarrow 0$, i.e. the speed of particle \mathcal{A} approaches the local speed of light and the worldline of \mathcal{A} approaches a null geodesic.

The Christoffel symbols in equation (8) are obtained from the metric tensor in Fermi coordinates

$$g_{00} = -1 - {}^FR_{0i0j}X^iX^j + O(|\mathbf{X}|^3), \quad (12)$$

$$g_{0i} = -\frac{2}{3} {}^FR_{0jik}X^jX^k + O(|\mathbf{X}|^3), \quad (13)$$

$$g_{ij} = \delta_{ij} - \frac{1}{3} {}^FR_{ikjl}X^kX^l + O(|\mathbf{X}|^3), \quad (14)$$

where

$${}^FR_{\alpha\beta\gamma\delta}(T) = R_{\mu\nu\rho\sigma}\lambda^\mu_{(\alpha)}\lambda^\nu_{(\beta)}\lambda^\rho_{(\gamma)}\lambda^\sigma_{(\delta)} \quad (15)$$

is the projection of the Riemann tensor on the orthonormal parallel-propagated tetrad frame $\lambda^\mu_{(\alpha)}$ along the worldline of \mathcal{O} . Here $\lambda^\mu_{(0)} = dx^\mu/d\tau$ is the four-velocity vector of \mathcal{O} and constitutes the temporal axis of its local frame while $\lambda^\mu_{(i)}$, $i = 1, 2, 3$, are the unit spatial axes that constitute the orthonormal spatial triad of the local frame such that

$$g_{\mu\nu}\lambda^\mu_{(\alpha)}\lambda^\nu_{(\beta)} = \eta_{\alpha\beta}. \quad (16)$$

Here $\eta_{\alpha\beta}$ is the Minkowski metric tensor with signature +2 and τ is the proper time of \mathcal{O} ; moreover, the Fermi system is so constructed that for this reference observer $(T, \mathbf{X}) = (\tau, \mathbf{0})$.

The infinite series in (12)–(14) consist of increasing powers of the relative distance with time-dependent coefficients that involve derivatives of the Riemann tensor along the worldline of \mathcal{O} . The general behavior of the higher-order terms has been discussed in [2, 6]; in fact, though the higher-order terms in (12)–(14) can be computed in principle, this has actually been done only up to the terms of order $|\mathbf{X}|^4$. The Fermi coordinates are admissible for $|\mathbf{X}| < \mathcal{R}$, where $\mathcal{R}(T)$ is the radius of the cylindrical region along the worldline of \mathcal{O} .

To determine \mathcal{R} , consider the nonzero components of the Riemann tensor and its covariant derivatives along the reference geodesic \mathcal{O} ; then, \mathcal{R} is defined to be

$$\inf \left\{ \frac{1}{|{}^F R_{\alpha\beta\gamma\delta}|^{1/2}}, \left| \frac{{}^F R_{\alpha\beta\gamma\delta}}{{}^F R_{\alpha\beta\gamma\delta,\rho}} \right|, \left| \frac{{}^F R_{\alpha\beta\gamma\delta,\rho}}{{}^F R_{\alpha\beta\gamma\delta,\rho\sigma}} \right|, \dots \right\}. \quad (17)$$

The relationship between \mathcal{R} and the radii of convergence of the series in (12)–(14) is not known.

Using the explicit form of the metric tensor in (12)–(14), equations (8) and (11) can be expressed as

$$\begin{aligned} & \frac{d^2 X^i}{dT^2} + {}^F R_{0i0j} X^j + 2 {}^F R_{ikj0} V^k X^j \\ & + \left(2 {}^F R_{0kj0} V^i V^k + \frac{2}{3} {}^F R_{ikjl} V^k V^l + \frac{2}{3} {}^F R_{0kjl} V^i V^k V^l \right) X^j + O(|\mathbf{X}|^2) = 0, \end{aligned} \quad (18)$$

and

$$\begin{aligned} \frac{1}{\Gamma^2} &= 1 - V^2 + {}^F R_{0i0j} X^i X^j + \frac{4}{3} {}^F R_{0jik} X^j V^i X^k \\ &+ \frac{1}{3} {}^F R_{ikjl} V^i X^k V^j X^l + O(|\mathbf{X}|^3) > 0. \end{aligned} \quad (19)$$

Equation (18) should be compared and contrasted with equation (2): There is no impediment in the gravitational case for changing the velocity of an ultrarelativistic particle with $|\mathbf{V}|$ initially very near unity in contrast with electrodynamics. Moreover, it follows from equation (5) that in the gravitational case, the analogue of the electromagnetic particle energy equation takes the form

$$\frac{1}{\Gamma} \frac{d\Gamma}{dT} = -\Gamma_{\alpha\beta}^0 \frac{dX^\alpha}{dT} \frac{dX^\beta}{dT}, \quad (20)$$

so that unlike the electrodynamic case, the rate of variation of particle energy is in fact proportional to the energy of the particle. For one-dimensional relative motion in the X direction with $V = dX/dT$, equation (18) reduces to

$$\frac{dV}{dT} + \kappa(1 - 2V^2)X + O(X^2) = 0, \quad (21)$$

where $\kappa = {}^F R_{TXTX}(T)$. Equation (21) should be compared and contrasted with equation (3). Neglecting higher-order terms in (21), we note the existence of a critical speed $V_c = 1/\sqrt{2} \approx 0.7$ in the gravitational case. The physics of this critical speed has been discussed in our

previous work [2, 3, 4, 5, 6]; indeed, the existence of the critical speed is basically due to the fact that the motion of \mathcal{A} is expressed with respect to the Fermi coordinate time T , which reduces to the proper time of the reference observer \mathcal{O} along its worldline.

Consider the solution of (21) with initial conditions that at $T = 0$, $X = 0$ and $V = \sqrt{\Gamma_0^2 - 1}/\Gamma_0$ such that $\Gamma_0 \gg 1$. Ignoring higher-order tidal terms, a simple integration of (21) demonstrates that depending on the sign and magnitude of κ , one can raise or lower the velocity V considerably. In fact, V can be raised to a value such that the quantity Γ^{-2} corresponding to equation (19), i.e.

$$\Gamma^{-2} = 1 - V^2 + \kappa X^2 + O(X^3), \quad (22)$$

vanishes provided that higher-order terms are neglected. This singular behavior signals the breakdown of the test particle approach adopted in our treatment, where higher-order tidal terms are perforce ignored. These issues will be illustrated in the next section in the context of the simplest gravitational field of astrophysical interest, namely, the exterior Schwarzschild spacetime. It turns out that the results are observationally significant only near gravitationally collapsed configurations.

II. TIDAL EFFECTS IN SCHWARZSCHILD SPACETIME

Imagine a swarm of relativistic particles around a point P in the exterior Schwarzschild spacetime that corresponds to the gravitational field of a mass M embedded in an otherwise flat spacetime with asymptotically inertial coordinates (t, x, y, z) . Let the radial line joining the center of the spherical symmetry to P be the z axis. Then in terms of the corresponding spherical polar coordinates (r, θ, ϕ) , the Schwarzschild metric is

$$-ds^2 = -\left(1 - \frac{2GM}{r}\right) dt^2 + \left(1 - \frac{2GM}{r}\right)^{-1} dr^2 + r^2(d\theta^2 + \sin^2\theta d\phi^2). \quad (23)$$

It is convenient to refer the motion of the particles in the swarm to an observer \mathcal{O} that starts from P at $r = r_0 > 2GM$ and moves relatively slowly along the radial z direction reaching infinity with a speed that is very small compared to unity. Our results turn out to be essentially independent of such a speed; therefore, we set it equal to zero for the sake of

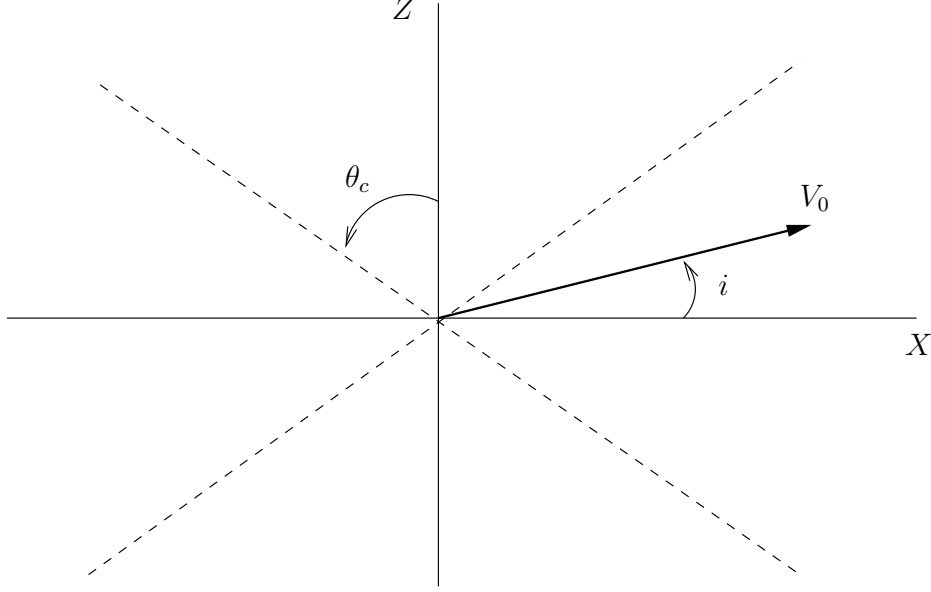


FIG. 1: Plot of the initial position and velocity of a particle in the Fermi coordinate system. The dashed lines represent the critical velocity cone demarcating the acceleration domains from the deceleration domains. The critical angle θ_c is given by $\tan \theta_c = 1/V_c = \sqrt{2}$, so that θ_c is approximately 54.7° .

simplicity. The geodesic path of \mathcal{O} is thus given by

$$\frac{dt}{d\tau} = \left(1 - \frac{2GM}{r}\right)^{-1}, \quad \frac{dr}{d\tau} = \sqrt{\frac{2GM}{r}}. \quad (24)$$

We then set up a Fermi coordinate system (T, X, Y, Z) about the worldline of \mathcal{O} such that $\lambda^\mu_{(3)}$ is along the radial direction. In fact, in the (t, r, θ, ϕ) coordinates we choose

$$\lambda^\mu_{(3)} = \left(\sqrt{\frac{2GM}{r}} \left(1 - \frac{2GM}{r}\right)^{-1}, 1, 0, 0\right). \quad (25)$$

There is then a rotational degeneracy in the choice of $\lambda^\mu_{(1)}$ and $\lambda^\mu_{(2)}$; once these vectors are chosen at a given instant of time, they are then parallel transported along the worldline.

The nonzero components of the Riemann tensor along the path of \mathcal{O} are given by

$${}^F R_{0101} = {}^F R_{0202} = -\frac{1}{2}k, \quad {}^F R_{0303} = k, \quad (26)$$

$${}^F R_{2323} = {}^F R_{3131} = \frac{1}{2}k, \quad {}^F R_{1212} = -k, \quad (27)$$

except for the symmetries of the Riemann tensor. Here k is given by

$$k = -\frac{2GM}{r^3}, \quad (28)$$

which can be expressed via the integration of (24) and $\tau \mapsto T$ as

$$k(T) = -2GM(r_0^{3/2} + \frac{3}{2}\sqrt{2GM}T)^{-2}. \quad (29)$$

More generally, the evaluation of equation (15) for an arbitrary timelike geodesic in Schwarzschild spacetime has been considered in [7].

The equations of motion of the particles in the swarm relative to \mathcal{O} are thus

$$\ddot{X} - \frac{1}{2}kX[1 - 2\dot{X}^2 + \frac{2}{3}(2\dot{Y}^2 - \dot{Z}^2)] + \frac{1}{3}k\dot{X}(5Y\dot{Y} - 7Z\dot{Z}) = 0, \quad (30)$$

$$\ddot{Y} - \frac{1}{2}kY[1 - 2\dot{Y}^2 + \frac{2}{3}(2\dot{X}^2 - \dot{Z}^2)] + \frac{1}{3}k\dot{Y}(5X\dot{X} - 7Z\dot{Z}) = 0, \quad (31)$$

$$\ddot{Z} + kZ[1 - 2\dot{Z}^2 + \frac{1}{3}(\dot{X}^2 + \dot{Y}^2)] + \frac{2}{3}k\dot{Z}(X\dot{X} + Y\dot{Y}) = 0, \quad (32)$$

together with the timelike condition, namely, that

$$\Gamma^{-2} = 1 - V^2 - \frac{1}{2}k(X^2 + Y^2 - 2Z^2) + \frac{1}{6}k[(\dot{X}Z - X\dot{Z})^2 + (\dot{Y}Z - Y\dot{Z})^2 - 2(\dot{X}Y - X\dot{Y})^2] \quad (33)$$

be positive. Here the overdot denotes differentiation with respect to the Fermi time T ; moreover, we have limited our attention to terms given explicitly in equations (12)–(14). Equations (30)–(32) and (33) can be put in dimensionless form if all spatial and temporal durations are expressed in units of GM . There is therefore a simple scaling law at work here for different mass scales (for instance, microquasars \rightarrow quasars). Our results are most important very near the source, since the tidal forces decrease as r^{-3} away from the source.

To simplify matters, we take advantage of the axial symmetry of this system about the Z direction and set $Y(T) = 0$ for all T . The resulting system can be integrated with the initial conditions that at $T = 0$, $X = Z = 0$ and

$$\dot{X} = V_0 \cos i, \quad \dot{Z} = V_0 \sin i, \quad (34)$$

where i is the inclination angle and V_0 is the initial speed $V_0 = \sqrt{\Gamma_0^2 - 1}/\Gamma_0$ such that $\Gamma_0 \gg 1$, see Fig. 1.

For the motion of a free test particle \mathcal{A} along the (radial) Z direction, $i = \pi/2$, the equations of motion (30)–(32) reduce to the nonlinear equation

$$\ddot{Z} + kZ(1 - 2\dot{Z}^2) = 0. \quad (35)$$

The main aspects of nonlinearity here that are significant for our discussion are the existence of critical solutions involving uniform motion at $V_c = \pm 1/\sqrt{2}$ and the effective change in

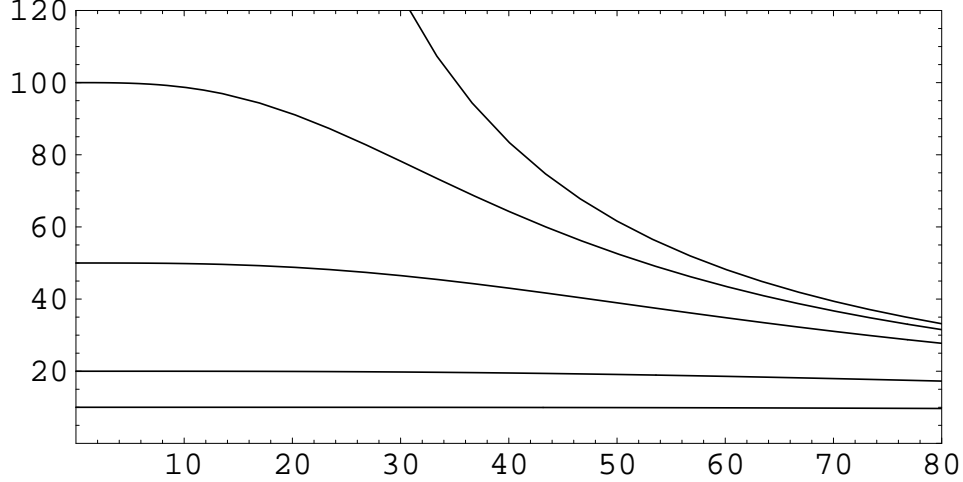


FIG. 2: Plot of the Lorentz factor $\Gamma = 1/\sqrt{1 - \dot{Z}^2 - 2GMZ^2/r^3}$ versus $T/(GM)$ based on the integration of equation (35) for $r_0 = 100 GM$ and $\Gamma_0 = 10, 20, 50, 100$ and 1000 .

the sign of curvature k for $\dot{Z}^2 > 1/2$. For initially ultrarelativistic motion (i.e. $V_0 > 1/\sqrt{2}$), the particle decelerates toward the terminal speed $1/\sqrt{2}$ as demonstrated in Fig. 2. The details of the deceleration process depend upon $r_0 > 2 GM$. However, it is important to point out a *general feature* of the tidal deceleration mechanism in the particular case under consideration in Fig. 2: the particle starts at $T = 0$ with $r_0 = 100 GM$, $Z = 0$ and $\dot{Z} > 1/\sqrt{2}$ and decelerates to $\Gamma < 40$ during a time $T \approx 80 GM$ *regardless* of the initial $\Gamma_0 \geq 50$. Thus, for $\Gamma_0 \rightarrow \infty$, “infinite” deceleration can occur in a relatively short period of time; however, in this limiting case the test particle approximation breaks down.

On the other hand, for motion along the X direction, $i = 0$, the equations of motion reduce to an equation similar to (35),

$$\ddot{X} - \frac{1}{2}kX(1 - 2\dot{X}^2) = 0, \quad (36)$$

except that an initially ultrarelativistic particle accelerates along directions normal to the jet direction as illustrated in Fig. 3. As before, the particle starts at $T = 0$ with $r_0 = 100 GM$, $X = 0$ and $\dot{X} > 1/\sqrt{2}$; the integration ends at T_{end} when $\Gamma \rightarrow \infty$. We note that T_{end} may occur outside the domain of validity of Fermi coordinates; however, as $\Gamma_0 \rightarrow \infty$, $X_{\text{end}} = X(T_{\text{end}}) \approx T_{\text{end}}$ tends to zero and one might expect that in this case the influence of the higher-order terms may be small. It is in fact possible to show that in this limit T_{end} approaches zero as $\Gamma_0^{-2/3}$. This is demonstrated in appendix A. It is necessary to remark here that for sufficiently large Γ_0 , the influence of the particle on the background geometry

can no longer be neglected and hence our treatment becomes invalid.

To discuss the physics of the tidal acceleration/deceleration phenomena, it is useful to have an invariant measure of the energy of the test particle \mathcal{A} . Let us therefore introduce a class of static observers with four-velocity U_R^μ in the Fermi coordinate system such that in the (T, X, Y, Z) coordinates

$$U_R^\mu(T, \mathbf{X}) = \left(\frac{1}{\sqrt{-g_{00}}}, 0, 0, 0 \right). \quad (37)$$

These fundamental observers associated with Fermi coordinates are in general accelerated; of course, one exception is the reference geodesic \mathcal{O} that is at rest at the spatial origin of the Fermi system. At any given event along the path of \mathcal{A} , the corresponding fundamental observer at that event measures the energy per unit mass of \mathcal{A} to be $\hat{\Gamma} = -g_{\mu\nu} U_R^\mu U^\nu$, or

$$\hat{\Gamma} = \left(\sqrt{-g_{00}} - \frac{g_{0i} V^i}{\sqrt{-g_{00}}} \right) \Gamma. \quad (38)$$

In the approximation scheme of this section, we have $\hat{\Gamma} = \sqrt{-g_{00}} \Gamma$, so that with

$$-g_{00} = 1 + \frac{GM}{r^3} (X^2 + Y^2 - 2Z^2), \quad (39)$$

$\hat{\Gamma}$ decreases in the deceleration case ($X = Y = 0$) and increases in the acceleration case ($Y = Z = 0$). Therefore, employing the invariant $\hat{\Gamma}$ instead of Γ would simply enhance these main results of the present section.

The integration of equations (33) in the (X, Z) plane shows that deceleration is maximum at $i = \pi/2$ and monotonically decreases with decreasing inclination until about 35° as demonstrated in Fig. 4. Moreover, acceleration is maximum at $i = 0$ and monotonically decreases away from the X axis, as demonstrated in Fig. 5, until about 35° when it turns into deceleration. This circumstance can be illustrated by means of the critical velocity cone in Fig. 1: a particle with velocity within the cone decelerates relative to \mathcal{O} , while a particle with velocity outside the cone accelerates relative to \mathcal{O} .

In this section, we have studied the solutions of the geodesic equation limited to the lowest-order tidal terms in an appropriately chosen Fermi coordinate patch. Of course, the equations of general relativity can be expressed with respect to any admissible system of coordinates. We choose a quasi-inertial Fermi normal coordinate system due to its correspondence with the analysis of observational data. Inside the Fermi coordinate patch, the geodesic equation is exact within the test particle approximation scheme. Thus the particle

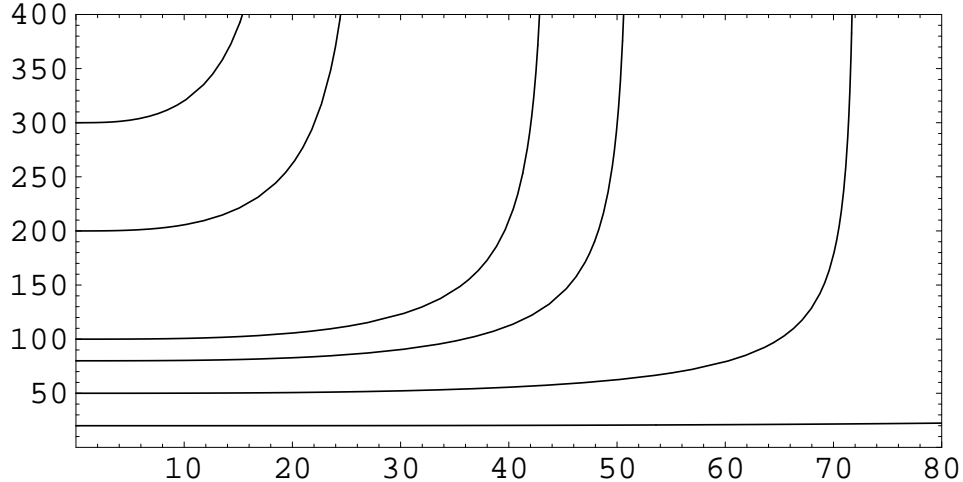


FIG. 3: Plot of the Lorentz factor $\Gamma = 1/\sqrt{1 - \dot{X}^2 + GMX^2/r^3}$ versus $T/(GM)$ based on the integration of equation (36) for $r_0 = 100 GM$ and $\Gamma_0 = 20, 50, 80, 100, 200$ and 300 .

velocity \mathbf{V} can take any value consistent with the equation of motion (18) and the time-like condition (19), see [5]. The Fermi coordinate system has been employed extensively in general relativity theory; for instance, it is used in [9] to discuss the local bending of light in a gravitational field. The robustness of our numerical results should be emphasized. In fact, our results do not change appreciably if instead of $\mathbf{X}(0) = 0$, the initial position of the test particle is chosen reasonably close to the reference observer. Moreover, the reference observer can be any relatively slow-moving test particle on a radial escape trajectory [6].

III. TIDAL ACCELERATION

This section is devoted to the singular phenomenon of tidal acceleration of particles to the local speed of light within the Fermi coordinate system as shown in Fig. 3. This singularity comes about due to the nonlinear character of equation (36): for $V > 1/\sqrt{2}$, the nonlinear factor $1 - 2V^2$ changes sign thereby leading to tidal acceleration. As Γ_0 increases, $T_{\text{end}}/(GM)$ decreases; the graph of $T_{\text{end}}/(GM)$ versus $\log_{10} \Gamma_0$ is given in Fig. 6. It follows from this figure that the singularity under consideration here is dynamic in origin and has nothing to do with the kinematic breakdown of the Fermi coordinate system for $|\mathbf{X}| \gtrsim \mathcal{R}$.

Imagine the general solution of the geodesic equation in the Fermi coordinate system in the (X, Z) plane, since the symmetry of the configuration permits us to set $Y(T) = 0$

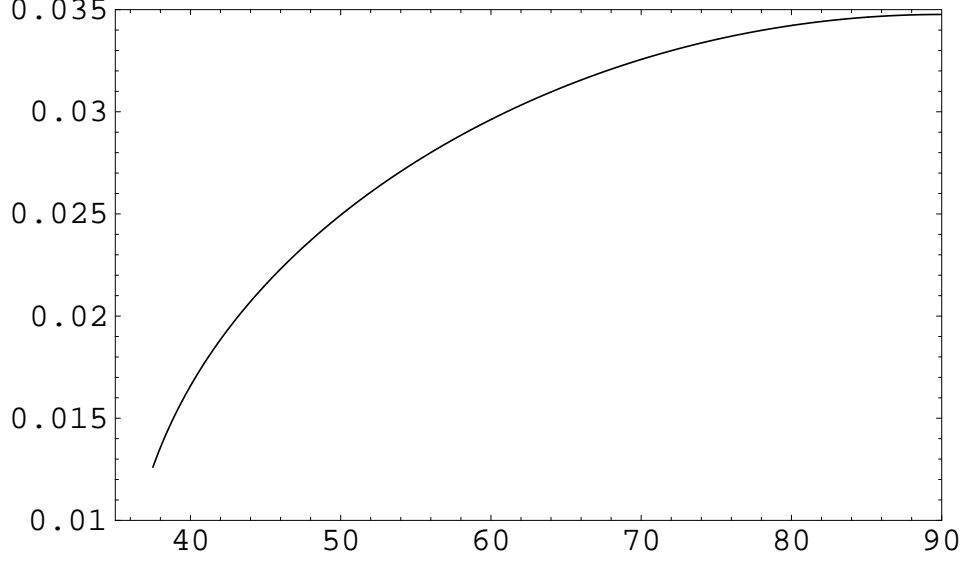


FIG. 4: Plot of GM/T_{dec} versus inclination angle i (measured in degrees in this figure) based on integration of equations (30)–(32) with initial data $X = Z = Y = 0$, $\dot{X} = V_0 \cos i$, $\dot{Y} = 0$, $\dot{Z} = V_0 \sin i$ and $r_0 = 100 GM$ at $T = 0$, where $V_0 = \sqrt{\Gamma_0^2 - 1}/\Gamma_0$ with $\Gamma_0 = 100$. The quantity T_{dec} is defined to be the duration of deceleration from $\Gamma_0 = 100$ to $\Gamma = 80$.

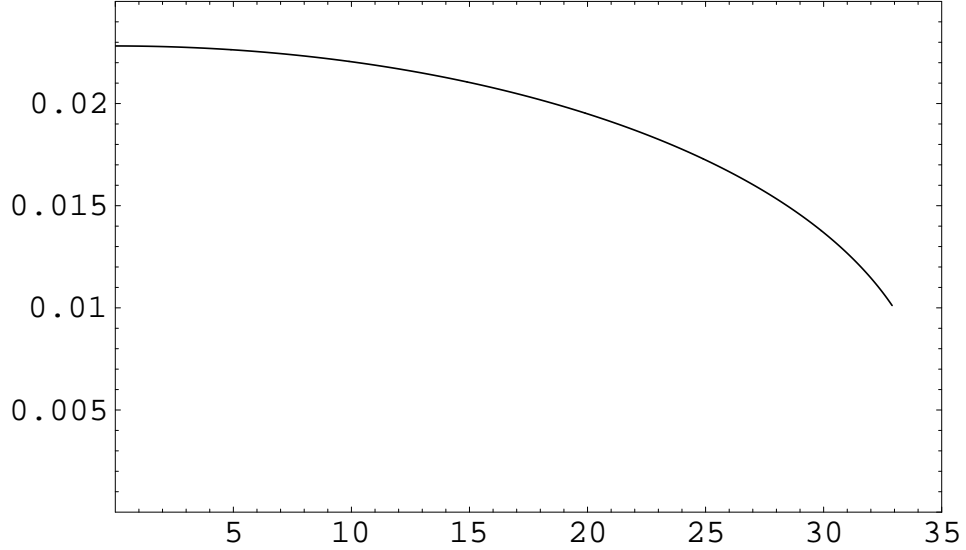


FIG. 5: Plot of GM/T_{end} versus inclination angle i (measured in degrees in this figure) based on integration of equations (30)–(32) with initial data $X = Z = Y = 0$, $\dot{X} = V_0 \cos i$, $\dot{Y} = 0$, $\dot{Z} = V_0 \sin i$ and $r_0 = 100 GM$ at $T = 0$, where $V_0 = \sqrt{\Gamma_0^2 - 1}/\Gamma_0$ with $\Gamma_0 = 100$.

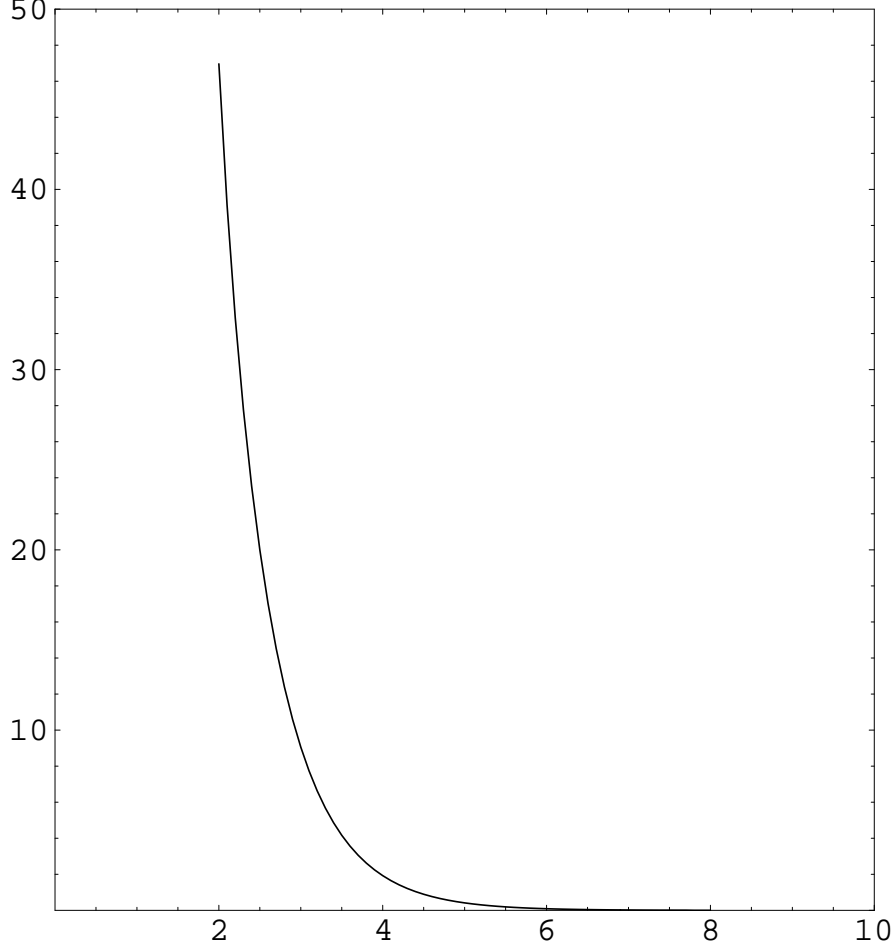


FIG. 6: Plot of $T_{\text{end}}/(GM)$ versus $\log_{10}(\Gamma_0)$ based on the integration of equation (36) with $r_0 = 100 GM$, $X = 0$ and $\dot{X} = \sqrt{\Gamma_0^2 - 1}/\Gamma_0$ at $T = 0$.

for all T . In this case, the generalization of the system (30)–(32) that takes into account second-order tidal terms [8] is given by

$$\ddot{X} + \frac{GM}{r^3} \left[X(1 - 2\dot{X}^2 - \frac{2}{3}\dot{Z}^2) + \frac{14}{3}\dot{X}Z\dot{Z} \right] = \frac{3GM}{2r^4} \left[2XZ(1 - 2\dot{X}^2 - \frac{1}{2}\dot{Z}^2) - (2X^2 - 5Z^2)\dot{X}\dot{Z} \right], \quad (40)$$

$$\ddot{Z} - \frac{2GM}{r^3} \left[Z(1 - 2\dot{Z}^2 + \frac{1}{3}\dot{X}^2) + \frac{2}{3}X\dot{X}\dot{Z} \right] = \frac{GM}{4r^4} \left[6X^2 - 12(1 - 2\dot{Z}^2)Z^2 - 20X\dot{X}Z\dot{Z} - 5Z^2\dot{X}^2 - 11X^2\dot{Z}^2 \right], \quad (41)$$

where we have employed the linear approximation scheme described in appendix B of [6] for the evaluation of the covariant derivatives of the Riemann tensor along the reference geodesic \mathcal{O} . In fact, the relevant nonzero covariant derivatives that are needed in the derivation of equations (40) and (41) are given by

$${}^F R_{1313,3} = -{}^F R_{0101,3} = -{}^F R_{0103,1} = \frac{1}{2} {}^F R_{0303,3} = 3 \frac{GM}{r^4}, \quad (42)$$

except for the symmetries of the curvature tensor. The timelike condition in this case takes the form

$$\begin{aligned} \frac{1}{\Gamma^2} = & 1 - \dot{X}^2 - \dot{Z}^2 + \frac{GM}{r^3} [X^2 - 2Z^2 - \frac{1}{3}(X\dot{Z} - Z\dot{X})^2] \\ & - \frac{GM}{r^4} [(3X^2 - 2Z^2)Z - \frac{1}{2}(X\dot{Z} + Z\dot{X})\dot{X}Z^2]. \end{aligned} \quad (43)$$

Moreover, $\hat{\Gamma} = \sqrt{-g_{00}} \Gamma$ in this approximation, where

$$-g_{00} = 1 + \frac{GM}{r^3}(X^2 - 2Z^2) - \frac{GM}{r^4}(3X^2 - 2Z^2)Z. \quad (44)$$

We integrate equations (40) and (41) with initial conditions that $X = Z = 0$ at $T = 0$ with $\dot{X} = V_0$ and $\dot{Z} = 0$; then, we use the results to plot the behavior of Γ and $\hat{\Gamma}$ versus $T/(GM)$. These plots turn out to be indistinguishable from figure 3, since the contribution of the second-order tidal terms is very small; in fact, for $\Gamma_0 = 50$, $T_{\text{end}}/(GM)$ turns out to be 72.14 for Γ and $\hat{\Gamma}$ compared with 72.12 in figure 3. Thus, the singularity in Γ is moderated by the presence of the higher-order terms.

These results follow from the integration of equations that are not the actual geodesic equation; indeed, the geodesic equation would contain the infinite set of higher-order tidal terms, whereas we have considered only the first and the second terms of this infinite set. Though the influence of each higher-order term by itself may be small, as we have just demonstrated in the case of the second-order terms, we cannot conclude that the same is necessarily true of the *whole* set. Physically, however, our results indicate that *with respect to the ambient medium* around the central source, the free particles of the swarm can undergo significant but finite tidal accelerations and decelerations depending upon their directions of propagation. The observational aspects of these results are discussed in the following section.

IV. DISCUSSION

In our work on the acceleration/deceleration phenomena, we have adopted an approach based on *relative* motion within a quasi-inertial reference frame (i.e. a Fermi normal coordinate system); in fact, this treatment is generally consistent with the analysis of observational data. Moreover, we have concentrated on geodesic, that is, force-free, flow for the swarm of particles. We have neglected plasma effects in this paper for the sake of simplicity; however, a more thorough investigation should certainly take these into account [11, 12]. Indeed, in the comparison of our theoretical results with observation, the astrophysical environment around the central source should play an important role.

It should be emphasized that the acceleration/deceleration phenomena that we have discussed occur within the Fermi coordinate system and are thus measurable relative to the ambient medium surrounding the central source. Let us note that at $T = 0$ and $r = r_0$, where the worldlines of \mathcal{O} and \mathcal{A} intersect,

$$\lambda^\mu_{(0)} U_\mu = -\Gamma_0, \quad \lambda^\mu_{(3)} U_\mu = \Gamma_0 V_0 \sin i. \quad (45)$$

These invariants can also be computed in the background Schwarzschild coordinate system and we find after a straightforward calculation that

$$\mathcal{E} = \left(1 + \sqrt{\frac{2GM}{r_0}} V_0 \sin i\right) \Gamma_0, \quad \mathcal{L} = r_0 \Gamma_0 V_0 \cos i, \quad (46)$$

where \mathcal{E} and \mathcal{L} are respectively the energy and orbital angular momentum per unit mass of the particle \mathcal{A} as determined by the static inertial observers at infinity in the exterior Schwarzschild spacetime. In fact, \mathcal{E} and \mathcal{L} are constants along the geodesic orbit of \mathcal{A} . Thus if this geodesic orbit actually escapes to spatial infinity ($\mathcal{E} \geq 1$), it would not appear to have any remarkable features as determined by the asymptotically static inertial observers; for example, for the accelerating particle discussed in section III, $\mathcal{E} = \Gamma_0$ and $\mathcal{L} = r_0 \Gamma_0 V_0$ since $i = 0$. On the other hand, if the motion of \mathcal{A} is referred to the ambient medium surrounding the central source, the acceleration/deceleration phenomena that we have discussed can be measured. This is the key point: the gain or loss of gravitational tidal energy is measurable *relative to the ambient medium*. In fact, the interaction of (charged) particles in the swarm with the ambient medium can lead to the radiation of tidal energy to distant observers. For instance, the collisions of such accelerated particles with those of the ambient medium can

transfer their tidal energies to the latter particles that could then escape from the system and appear far away as highly energetic cosmic rays.

The acceleration phenomena are consistent with the recent observations—by the *Chandra* X-Ray Observatory [13]—of accelerated motion normal to the jet directions in four neutron stars in our galaxy: Crab Pulsar, Vela Pulsar, PSR B1509-58 and SNR G54.1+0.3. A detailed analysis of the recent Crab nebula X-ray data is contained in [14, 15]. The deceleration phenomena are consistent with observations of the speed of the plasma clumps in microquasar jets [16]. Our theoretical assumptions rely upon the analysis of such observations based on the detection of relative motion using the standard flat geometry of an inertial system of coordinates. Indeed, the acceleration of particles normal to the jet direction is measured relative to the fixed central features associated with the jets near the source [13]. Moreover, the motion of a clump within a jet is measured relative to certain “fixed” features of the ambient medium [16].

What is the source of energy for the gravitational acceleration of particles? While a local description of gravitational energy is not possible in accordance with Einstein’s principle of equivalence, we must nevertheless account for the energy of the swarm of particles as measured by the ambient medium around the source. Ultrarelativistic particles moving away from the source within the critical velocity cone *lose* energy and approach the critical speed regardless of their initial ultrarelativistic speed. On the other hand, ultrarelativistic particles moving outside the critical velocity cone *gain* energy and accelerate as they move outward. We expect that there is essentially a balance between the energies that are lost and gained in the deceleration and acceleration processes, respectively. If the net energy that leaves the system is positive, one may speculate that the whole system of particles around the source would slightly shrink. Such a contraction would lead to the release of gravitational energy that could account for the net loss of energy to the highly energetic particles that leave the system; however, the detailed dynamics as well as the limitations of such processes is beyond the scope of this work.

The rotation of the central source has been neglected in this paper; however, detailed studies have revealed that—other than specifying the jet directions—the influence of the rotation of the central source on our specific acceleration/deceleration results is rather small [2, 3, 4, 5, 6].

Finally, we should mention that UHE cosmic rays of energy $\sim 10^{20}$ eV are not expected

to reach the Earth from extragalactic sources due to the GZK effect [17, 18, 19]. Our acceleration results indicate that the observed UHE cosmic rays may come from microquasars or neutron stars in our galaxy. This idea could be tested with the Pierre Auger Observatory [20].

APPENDIX A

The purpose of this appendix is to study the behavior of T_{end} as $\Gamma_0 \rightarrow \infty$; indeed, we will show that in this limit $T_{\text{end}} \propto \Gamma_0^{-2/3}$. As in the numerical work reported in this paper, we will consider the solution $X(T, V_0)$ of the differential equation

$$\ddot{X} = -\frac{GM}{r^3}X(1 - 2\dot{X}^2) \quad (\text{A1})$$

with initial conditions $X(0, V_0) = 0$ and $V(0, V_0) = V_0$, and

$$\frac{1}{\Gamma^2} = 1 - V^2 + \frac{GM}{r^3}X^2. \quad (\text{A2})$$

We note that the solution of the differential equation has continuous partial derivatives of all orders with respect to T and V_0 by standard results in the theory of ordinary differential equations (see [10]).

Since $\Gamma \rightarrow \infty$ if and only if the right-hand side of equation (A2) vanishes, we define

$$\Upsilon(T, V_0) := 1 - V(T, V_0)^2 + \frac{GM}{r(T)^3}X(T, V_0)^2 \quad (\text{A3})$$

and discuss the equation $\Upsilon(T, V_0) = 0$.

Let us observe that $\Upsilon(0, 1) = 0$. That is, $\Gamma = \infty$ for a particle whose initial velocity at $X = 0$ is the speed of light. We will show that there is a *unique* implicit solution $V_0(T)$ (i.e. $\Upsilon(T, V_0(T)) = 0$) such that $V_0(0) = 1$ and $V_0(T) < 1$ for T near $T = 0$. Moreover, for $T > 0$ and near $T = 0$, the implicit solution can be inverted so that $\Upsilon(T(V_0), V_0) = 0$; that is, for each extremely ultrarelativistic solution, there is a finite time—previously denoted as T_{end} —depending on the initial velocity V_0 such that $\Gamma \rightarrow \infty$. Also, $T(V_0)$ is a decreasing function of V_0 such that $T(V_0) \rightarrow 0$ as $V_0 \rightarrow 1$.

The proof of these statements is simply an application of the implicit function theorem. Note that $\Upsilon(0, 1) = 0$ and $\Upsilon_{V_0}(0, 1) = -2$; therefore, by the implicit function theorem, there is a function $V_0(T)$ defined for T near $T = 0$ such that $\Upsilon(T, V_0(T)) = 0$ and if $\Upsilon(T^*, V_0^*) = 0$

for (T^*, V_0^*) near $(0, 1)$, then $V_0(T^*) = V_0^*$. To demonstrate that for $T > 0$ the curve $(T, V_0(T))$ lies in the physical region ($V_0(T) < 1$), we will show that the Taylor series of V_0 centered at $T = 0$ is given by

$$V_0(T) = 1 - \frac{1}{\sqrt{2}}(GM)^{3/2}r_0^{-9/2}T^3 + O(T^4). \quad (\text{A4})$$

In fact, the remaining claims are all simple consequences of this result.

To establish equation (A4), we first note that

$$r(T) = (r_0^{3/2} + \frac{3}{2}\sqrt{2GM}T)^{2/3} \quad (\text{A5})$$

and $\ddot{X}(0, 1) = 0$. A simple computation yields $\Upsilon_T(0, 1) = 0$, and, from differentiating $\Upsilon(T, V_0(T)) = 0$, that is,

$$\Upsilon_T(T, V_0(T)) + \Upsilon_{V_0}(T, V_0(T))V_0'(T) = 0, \quad (\text{A6})$$

we conclude that $V_0'(0) = 0$, where the prime denotes differentiation of the function V_0 . Proceeding in the same manner to compute the higher-order derivatives of $V_0(T)$, we find that $V_0''(0) = 0$ and then differentiating equation (A6) twice leads to

$$V_0'''(0) = \frac{1}{2}\Upsilon_{TTT}(0, 1). \quad (\text{A7})$$

Next, differentiating equation (A1) twice with respect to time leads to

$$X_{TTT}(0, 1) = \frac{GM}{r_0^3}, \quad X_{TTTT}(0, 1) = 2W, \quad (\text{A8})$$

where W is given by

$$W = \frac{d}{dT}\left(\frac{GM}{r^3}\right)\Big|_{T=0} = -3\sqrt{2}\left(\frac{GM}{r_0^3}\right)^{3/2}. \quad (\text{A9})$$

Moreover, it follows from differentiating equation (A3) three times with respect to T that

$$\Upsilon_{TT}(0, 1) = 0, \quad \Upsilon_{TTT}(0, 1) = -2X_{TTTT}(0, 1) + 6W. \quad (\text{A10})$$

Therefore, $X_{TTTT}(0, 1) = \Upsilon_{TTT}(0, 1) = 2W$ and $V_0'''(0) = W$, as required.

Starting from equation (A4), we can now derive a simple approximate relationship between Γ_0 and $T_{\text{end}}/(GM)$ that is valid for extremely ultrarelativistic particles:

$$\left(\frac{T_{\text{end}}}{GM}\right)^3 \approx \frac{1}{\sqrt{2}}\left(\frac{GM}{r_0}\right)^{-9/2}\Gamma_0^{-2}. \quad (\text{A11})$$

Thus for $r_0 = 100GM$ and $\Gamma_0 = 300$ we find $T_{\text{end}}/(GM) \approx 20$, in agreement with the numerical results of Fig. 6.

-
- [1] J. L. Synge, *Relativity: The General Theory* (North-Holland, Amsterdam, 1960).
 - [2] C. Chicone and B. Mashhoon, *Class. Quantum Grav.* **19**, 4231 (2002).
 - [3] C. Chicone, B. Mashhoon and B. Punsly, *Int. J. Mod. Phys. D* **13**, 945 (2004).
 - [4] C. Chicone and B. Mashhoon, *Class. Quantum Grav.* **21**, L139 (2004).
 - [5] C. Chicone and B. Mashhoon, *Class. Quantum Grav.* **22**, 195 (2005).
 - [6] C. Chicone and B. Mashhoon, *Ann. Phys. (Leipzig)* **14**, 290 (2005).
 - [7] J. D. Finley III, *J. Math. Phys.* **12**, 32 (1971).
 - [8] B. Mashhoon, *Astrophys. J.* **216**, 591 (1977).
 - [9] J. Ehlers and W. Rindler, *Gen. Rel. Grav.* **29**, 519 (1997).
 - [10] C. Chicone, *Ordinary Differential Equations with Applications* (Springer, New York, 1999).
 - [11] B. Punsly, *Black Hole Gravitohydromagnetics* (Springer-Verlag, New York, 2001).
 - [12] A. W. Guthmann, M. Georganopoulos, A. Marcowith and K. Manolaku, eds., Relativistic Flows in Astrophysics, *Lect. Notes Phys.* **589** (Springer, Berlin, 2002).
 - [13] <http://chandra.harvard.edu/photo/chronological.html>.
 - [14] S. Shibata, H. Tomatsuri, M. Shimanuki, K. Saito and K. Mori, *Mon. Not. R. Astron. Soc.* **346**, 841 (2003).
 - [15] K. Mori, D. N. Burrows, J. J. Hester, G. G. Pavlov, S. Shibata and H. Tsunemi, *Astrophys. J.* **609**, 186 (2004).
 - [16] R. Fender, in *Compact Stellar X-ray Sources*, eds. W. H. G. Lewin and M. van der Klis (Cambridge University Press, Cambridge, 2004).
 - [17] K. Greisen, *Phys. Rev. Lett.* **16**, 748 (1966).
 - [18] G. T. Zatsepin and V. A. Kuzmin, *JETP Lett.* **4**, 78 (1966) [*Pisma Zh. Eksp. Teor. Fiz.* **4**, 114 (1966)].
 - [19] D. F. Torres and L. A. Anchordoqui, *Rep. Prog. Phys.* **67**, 1663 (2004).
 - [20] <http://www.auger.org>.